Extracting Flame Describing Functions in the Presence of Self-Excited Thermoacoustic Oscillations

Saravanan Balusamy[a,*], Larry K B Li[b], Zhiyi Han[c], Simone Hochgreb[c]

Colloquium: *Gas Turbine Combustion*

Paper length: *Method 2 (two columns): 6.5 pages × 900 words/page = 5850 words*

[a]*Department of Mechanical and Aerospace Engineering, Indian Institute of Technology Hyderabad, Kandi, Sangareddy - 502285, INDIA*
[b]*Department of Mechanical and Aerospace Engineering, The Hong Kong University of Science and Technology, Clear Water Bay, Kowloon, Hong Kong*
[c]*Department of Engineering, University of Cambridge, Trumpington Street, Cambridge, CB2 1PZ, UK*

Abstract

One of the key elements in the prediction of thermoacoustic oscillations is the determination of the acoustic response of flames as an element in an acoustic network, in the form of a flame describing function (FDF). In order to obtain a response, flames often have to be confined into a system with its own acoustic response. Separating the pure flame response and that of the system can be complicated by the non-linear effects that the flame can have on the overall system response. In this paper, we investigate whether it is possible to obtain a flame response via the usual methods of dynamic chemiluminescence and pressure measurements, starting from an unforced system with incipient self-excitations at a given frequency f_s, in the form of a stabilized flame at atmospheric pressure with a 700 mm tube as a combustor. The flame is forced at discrete frequencies from 20 to 400 Hz, away from the self-excitation, and the response of the flame is measured using OH* chemiluminescence. This response was compared to a flame response measured in a short tube with no other excitations.

The results show that both the gain and phase can be entirely dominated by the behavior of the self-excitation, so that in general it is not possible to extract reliable gain and phase information as if the forced and self-excited modes acted independently and linearly. Although the gain in this particular case was not significantly affected, the phase information of the original flame became dominated by the triggered self-excitation. Boundary conditions and systems used for flame acoustic forcing therefore need to be carefully controlled whenever there is a possibility of self-excitation.

Keywords: Thermoacoustics, Nonlinear dynamics, Combustion instability, Turbulent premixed flames, Self-excited oscillations

1. Introduction

The principles that give rise to thermoacoustic oscillations in combustors have been known for over a century [1], but the methods of prediction of both the frequency and amplitude of such oscillations continue to be developed. Over the past twenty years, significant advances have been made in the use of nonlinear methods for quantitative prediction [2–6]. The overall behavior of the system has been shown to be reasonably accurately captured by a combination of acoustic network modeling, nonlinear flame describing functions (FDFs), and in some cases, entropy describing functions [7]. These functions are the gain and phase in heat release rate or entropy, respectively, due to the change in another scalar, typically the acoustic velocity perturbation.

Significant work has therefore been devoted to developing methods for measuring FDFs in a variety of flames. Most experimental rigs involve a method for forcing the input, typically via a loudspeaker or siren, while the flame response is measured via chemiluminescence of OH* or CH*, which have been shown to correlate linearly with the rate of heat release in premixed flames [8, 9]. Experiments by Ćosić *et al.* [6] and earlier by Schuermans *et al.* [10] showed that it is also possible to experimentally obtain FDFs by measuring the transfer functions of acoustic waves across a flame via use of the multiple microphone method (MMM). These results were shown to approximate well the flame transfer functions (FTFs) measured using chemiluminescence under premixed conditions. Although the method requires an estimate of the post-flame temperatures, the key advantage is that it enables the measurement of FTFs under partially premixed conditions, where chemiluminescence measurements may be unreliable. The method demonstrated by Ćosić *et al.* [6] was deployed in a well controlled experiment at atmospheric conditions, with variable length sections both upstream and downstream of the flame. Previous work by Schuermans *et al.* [10] also used the same method in a high pressure combustor with a nearly anechoic (non-reflecting) downstream boundary. In many practical situations, however, such ideal conditions may not be produced, as it is often laborious and expensive to invest in large facilities with controlled boundaries at high pressure, or with long extensible moving sections.

In those situations, self-excited oscillations at a particular

*Corresponding author
Email address: saravananb@iith.ac.in (Saravanan Balusamy)

frequency may develop naturally at selected operating conditions, as a result of the nonlinear combination of boundary and operating conditions, and the very FDFs one wishes to measure. Such FDFs have in the past been extracted using high pressure facilities [11, 12], even though a self-excited instability was present in the system at a particular frequency range. Previous work by Balusamy *et al.* [13] showed how forced oscillations under these conditions can excite or suppress natural self-excited oscillations. Experiments by Balachandran *et al.* [14] showed nonlinear interactions between two forcing frequencies, and the work by Schimek *et al.* [15] demonstrated the effect of forcing a system off its natural frequencies, but neither group compared their results to that of a system that was not self-excited. Finally, work by Moeck and Paschereit [16] and Bothien *et al.* [17] offered a comprehensive analysis of nonlinear interactions of multiple modes based on existing models of system nonlinear dynamics and control, offering a number of explanations for the findings in [14, 15], and demonstrated the use of active changes in boundary conditions to control the onset of oscillations. In the present experiments, we consider the question of whether and how the response of a flame at the forcing frequency is affected by the presence of low level self-excited oscillations, to understand how these may affect measurements of flame response function in realistic systems.

2. Experimental setup

Experiments are performed on an axisymmetric swirl-stabilized burner (Fig. 1), which has been used before to study the forced response of stratified flames [18] and the interaction between forcing and self-excitation in premixed flames [13, 19, 20].

For this paper, premixed flames are created by mixing air and methane, both metered with mass flow controllers (Alicat MCR series, ± 0.2% FS). This reactant mixture is split into two streams that enter the mixing plenum via either a graduated bypass valve, or via a siren. The siren consists of a stator and a rotor, whose rotational speed determines the forcing frequency, as controlled by a variable-speed motor (EZ motor Model 55EZB500). The forcing amplitude is independently controlled by varying the opening of the graduated bypass valve.

The mixing plenum is 1000 mm long and consists of two concentric tubes (diameters: 15.05 and 27.75 mm) and an axisymmetric centerbody (diameter: 6.35 mm). The downstream ends of both tubes are aligned flush with the end of the centerbody. For flame stability, two axial swirlers are mounted in each annular section. Each swirler has six swirl vanes, of thickness 0.5 mm, aligned at 45° to the flow. Downstream of the burner exit is the combustor, which consists of a stainless steel base plane and an optically accessible fused-silica tube of 94 mm diameter. Both a short tube (150 mm) and a long tube (700 mm) are used during the forced experiments. The exit of this tube is at ambient conditions. For certain flame conditions, the long combustor geometry supports thermoacoustically self-excited oscillations at the fundamental (longitudinal) mode of the tube. No self-excited oscillations are observed for the short tube.

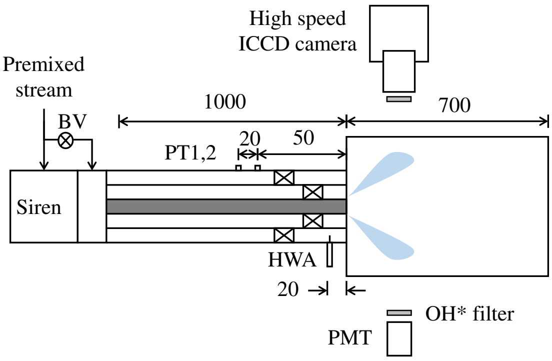

Figure 1: Schematic of the swirl-stabilized turbulent premixed burner. BV: bypass valve, PT: pressure transducer, PMT: photomultiplier tube, HWA: hot-wire anemometer

These oscillations are examined by measuring the dynamic pressure in the mixing plenum with two pressure transducers, mounted upstream (Model 40BP GRAS), at 70 and 50 mm (PT1,2) upstream of the combustor inlet. From these, the acoustic velocity fluctuation upstream is calculated using the two-microphone method (TMM) [21]; the TMM velocities are proportional to but lower than those measured using hot-wires 20 mm upstream of the combustor inlet under non-reacting conditions, as the latter include further turbulent disturbances arising from the swirler boundary layers.

Chemiluminescence of excited OH* is measured using a photomultiplier tube (PMT, Thorlabs model PMM01) fitted with a bandpass filter (308 ± 10 nm). The chemiluminescence emission has been assumed to be proportional to the total heat-release rate [9, 22, 23]. At each test point, the pressure and PMT data are sampled at a frequency of 8192 Hz for 4 s on a data acquisition system (National Instruments, BNC-2111), resulting in a spectral resolution of 0.25 Hz and a temporal resolution of 0.122 ms. All of the experiments are performed at ambient temperature (T_a = 293 K) and atmospheric pressure.

The spatial distribution of heat release rate is examined by capturing OH* chemiluminescence images of the flame using a high-speed CMOS camera (Photron FASTCAM SA1.1) fitted with a gated intensifier (UVi2550-10S20, Invisible vision), an objective UV lens (Nikon Rayfact UV-105 mm f/4.5), and a bandpass filter (FGUV11, Thorlabs, 275-375 nm). The intensifier converts the UV signal of OH* chemiluminescence around 309 nm to visible signal linearly over a wide dynamic range, which is then amplified and acquired by the high-speed CMOS sensor. At each test point, a total of 4096 images are acquired with an exposure time of 50 μs, a frame rate of 2000 frames/second for long tube experiments and a frame rate of 8000 frames/second for short tube experiments with an image resolution of 896 × 752 pixels. These images are then post-processed by subtracting the background noise, by phase-averaging to generate line-of-sight Abel inverted images of the flame structure.

Table 1: Operating conditions

Parameter	Case 1	Case 2
u (m/s)	5	10
Q (kW)	6.8	13.6
f_s (Hz)	161 ± 4	190 ± 3
u'/u (%)	1.2 ± 0.5	6 ± 1.5
p'/p (%)	0.01 ± 0.005	0.1 ± 0.03
q'/q (%)	1 ± 0.4	4 ± 0.8

3. Results and discussion

3.1. Interaction between forcing and self-excitation

Tests performed without forcing show several unforced operating conditions capable of supporting self-excited instability. We focus on two of those operating conditions: Table 1. For both conditions, the equivalence ratio is $\phi = 0.8$ and the system exhibits self-excited limit-cycle oscillations at a natural frequency (f_s) that is lower than the expected frequency of the quarter-wave mode based on the combustor length at adiabatic temperatures, indicating coupling with the inlet duct.

The system is forced over a range of frequencies, but the interaction between the forcing and the system means that the achievable forcing amplitudes vary with frequency according to the joint modes of the inlet tube and combustor, as shown in Fig. 2. There are peaks around 40, 180 and 400 Hz during self excitation. These are close to the modes found during cold operation in the short tube, which are at 60, 160 and 380 Hz, which are chosen for scans of the flame response at different forcing amplitudes. These frequencies are selected for further analysis.

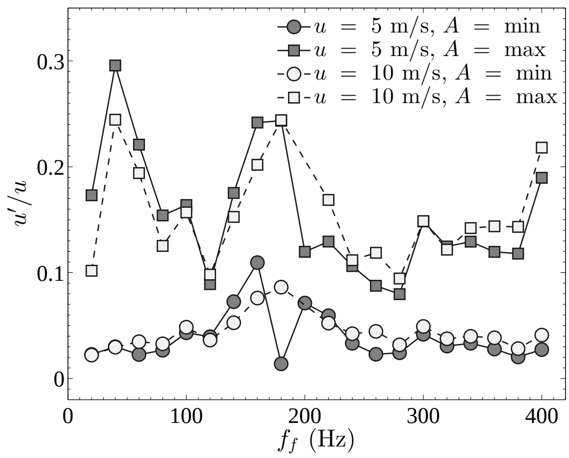

Figure 2: Summary of the forcing amplitudes ($A \equiv u'/u$) and forcing frequencies (f_f) investigated for both low power (u = 5 m/s) and high power (u = 10 m/s) case. At each f_f, A is varied from minimum to maximum.

Figure 3 shows the power spectrum of pressure and heat release rate for the operating cases considered. The amplitudes are changed across the range and frequencies shown in Fig. 2. The spectral characteristics have been analysed using several algorithms, including Hilbert and Welch. However, the most unambiguous representations were obtained using the FFT (with symmetric Hanning window of 32768 width) algorithm, as shown in Fig. 3. At low power (u = 5 m/s), the unforced oscillation at 161 Hz is just about detectable, but is triggered by forcing at 60 Hz forcing at an amplitude A=0.05 into a stronger self-excited oscillation at a slightly higher frequency. As the forcing amplitude increases, however, the system transitions from a periodic self-excitation to a quasi-periodic oscillation at the highest forcing amplitude, showing the combination of the two frequencies. The heat release fluctuations reflect the pressure changes, but their relative magnitude of the forced and self-excited perturbations are very different.

For forcing at 160 Hz (middle column), the self-excitation at 161 Hz becomes coherent with the forced mode, leading to system resonance and excitation, which shows up on the heat release rate as well as pressure. Finally, for the weaker available forcing at 380 Hz, the subharmonic of the forcing (at 190 Hz) triggers the self-excitation near 161 Hz, which moves up to the subharmonic frequency of 190 Hz, and produces an extra peak corresponding to the difference of 30 Hz between the subharmonic and the original self-excitation. Only the subharmonic appears to be present in the heat release plots.

Both the triggering and suppression behavior, as well as the frequency shift towards the right, have been discussed in [13] as being characteristic of non-linear model oscillators. In the present context, it is clear that (a) part of the energy input to the forced oscillation is diverted into lowering the self-excitation at the natural frequency, so one might expect that the forced behavior in the presence of a self-excitation should lead to lower flame response, and (b) an initially weak self-excitation can be triggered into a strong self-excitation, and this may affect the measured flame transfer function in systems that initially display no inherent oscillations.

At high power (bottom rows, u = 10 m/s), we see behavior similar to that at low power for both 60 and 160 Hz forcing frequencies, but the 380 Hz subharmonic now appears to suppress the self-excitation at 195 Hz when the forcing amplitude is large, with the 380 Hz component itself becoming more pronounced.

At high power (bottom row, u = 10 m/s), the incipient self excitation at 195 Hz is stronger at zero excitation. Forcing at 60 Hz triggers a much stronger excitation as measured by the pressure, albeit not reflected at the same magnitude in the heat fluctuation plot. Further increases in amplitude then suppress the self excitation, down to much lower levels. At 160 Hz forcing, we have a noticeable self-excitation which is completely suppressed with the addition of forcing at 160 Hz, which is not far from the self-excitation. Finally, at 380 Hz the self-excitation is again suppressed by the harmonic frequency at 190 Hz. This suppression has been discussed in previous papers, and explained in the context of non-linear system behavior [13]. Similar behavior is also noticed by [16] in the context of an analytical model for two-frequency forcing. In that paper, it is highlighted that this behavior is well known in control theory, and extensively used to control nonlinear oscillators by injection of high-frequency open-loop signals.

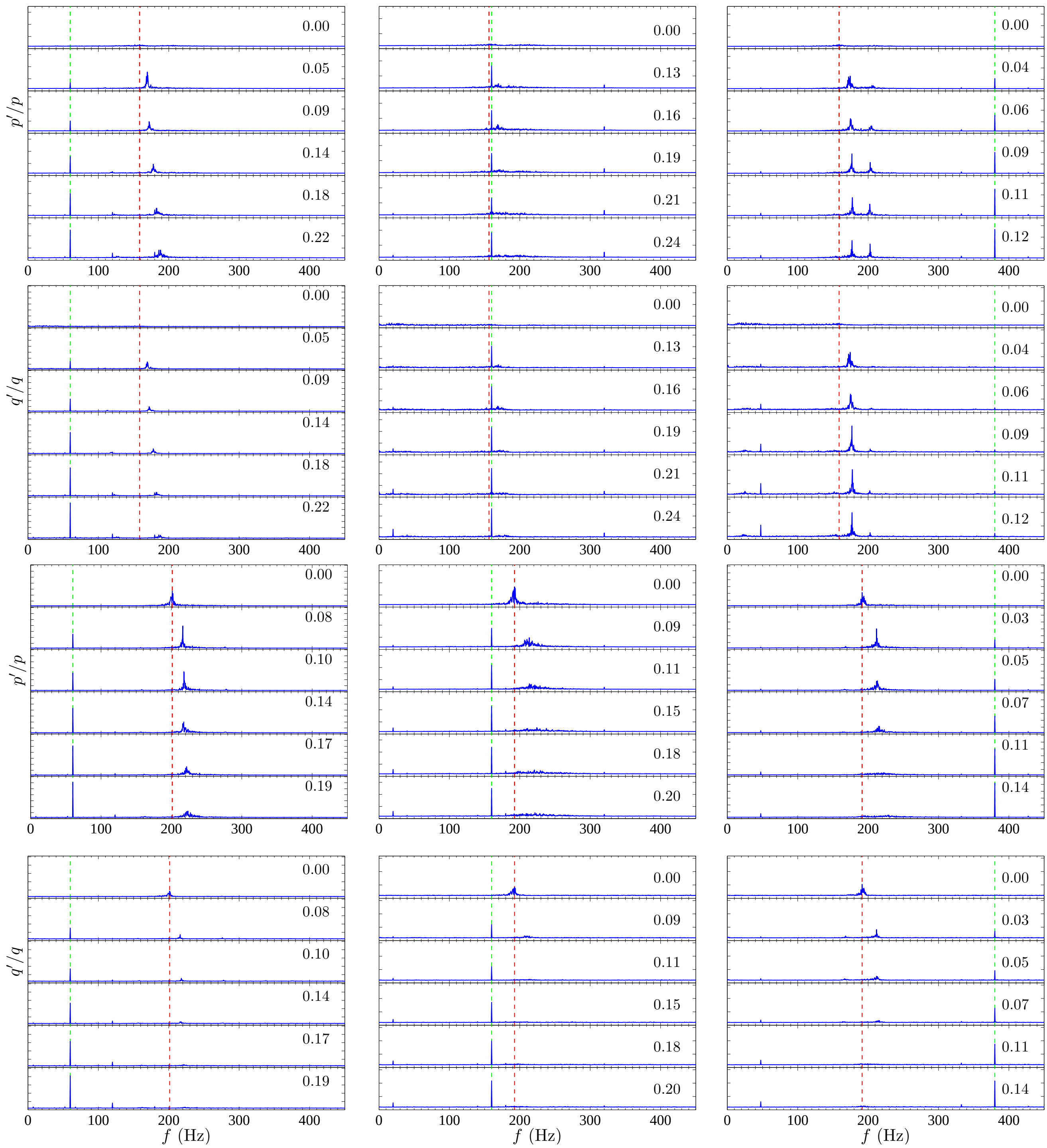

Figure 3: First and second row: u = 5 m/s. Third and fourth row: u = 10 m/s. Left column: f_f = 60 Hz, middle column: f_f = 160 Hz, right column: f_f = 380 Hz. Top and third row: Normalized spectrum of pressure signal P1: each division is 0.05%. Second and bottom row: Normalized OH* chemiluminescence spectrum q'/q: each division is 0.05. Forcing amplitude A as indicated. The dashed red line indicates the frequency of the emerging self-excitation in the absence of forcing, based on pressure. The dotted green line indicates the forcing frequency as determined from the pressure traces. (Figure is provided in color online.)

3.2. Flame Describing Functions

The response of the self-excited system under various forcing frequencies is captured as relative fluctuations in the heat release for a given velocity fluctuation, and the corresponding gain and phase difference between them (Fig. 4), where the frequency is varied in steps of 20 Hz and the siren bypass flow varied from minimum to maximum. The size and color of the markers indicate the forcing amplitude (A).

Considering the velocity oscillations for a sweep of siren frequencies in the low power case (5 m/s, top), we observe that the system resonances appear at 40, 180-190 and 400 Hz, as noted in (Fig. 2), and we recall that the system self-excitation appears at 165 Hz, which is pushed to a higher excitation of 180 Hz after triggering.

The intensity of the heat release at the forcing frequency rate largely mirrors that of the velocity. For each frequency, the increase is approximately linear for most frequencies. At the lowest intensities, the resulting gain oscillates, with peaks and troughs below 200 Hz, and a highly nonlinear gain at the triggered excitation around 180 Hz – clearly we are taking the overall gain at the frequency where both excited and forced frequencies contribute, so even a small velocity amplitude forcing is not necessarily related to the very large gains observed. The gain reaches an apparent node around 200 Hz, then recovers up to 260 Hz before decaying again at higher frequencies. The phase increases continuously from a phase difference of π at zero frequency, with a slope corresponding to the time delay between reference velocity and flame centroid, up to 180 Hz, where a sudden change in phase takes place, hopping by about π as the frequency sweeps the resonance.

At high power (u = 10 m/s), the self-excitation frequency appears around 195 Hz. Unlike the low power case, in which the major changes in behavior take place at 180 Hz, and the self-excitation frequency is at 165 Hz, the sudden change in behavior appears around the self excitation frequency of 195 Hz, and the flame response at f_f = 200 Hz is not included in those plots, as it exceeded the limits of the system operation. Again, we can see that the system behaves differently depending on whether it is forced above or below its self-excitation frequency: at low frequencies, the gain decreases up to 100 Hz, oscillating up and down to around 180 Hz. The phase rises from π at zero frequency up to almost 2π around 200 Hz, again with a slope with frequency corresponding to the acoustic delay time between excitation and flame, where it experiences a sudden change in phase of around π, again, then recovering back to a the same constant slope at higher frequencies.

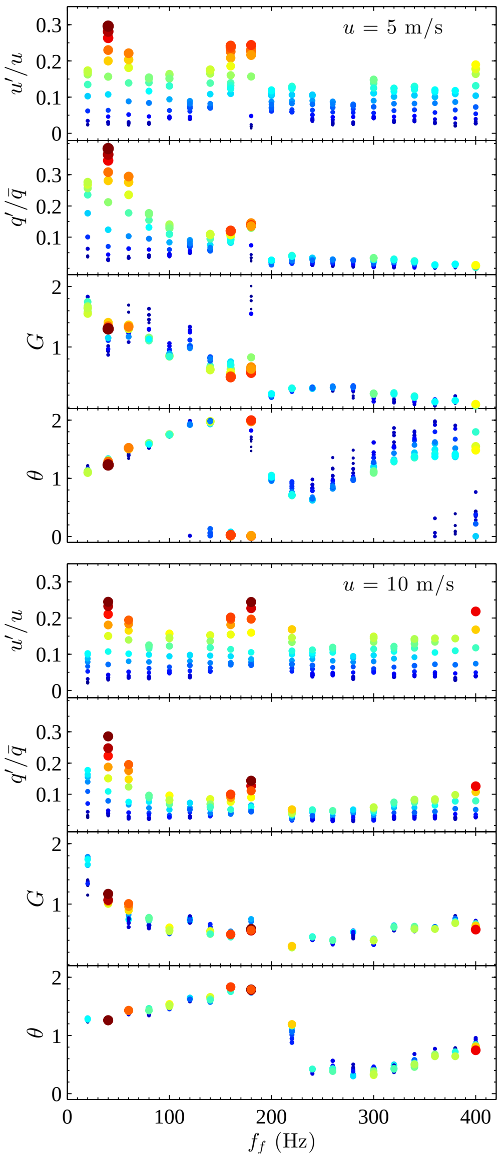

Figure 4: FDFs obtained for the long tube. Top: Forcing amplitudes. Second: normalized heat release fluctuation. Third row: gain. Bottom row: phase difference in multiples of π. The size and color of the markers indicate the forcing amplitude (A) as indicated in the top rows of low power and high power cases, respectively. (Figure is provided in color online.)

3.3. Long Tube vs. Short Tube

Figure 5 shows the heat release rate, gain and phase for increasing forcing amplitudes at the selected frequencies of 60, 160 and 380 Hz for which curves of gain as a function of amplitude for the current experiment, and the corresponding values for the short tube, non-excited case. Values are shown only for the higher power case, as extracted from the values in Fig. 4. The lower power case (u = 5 m/s) shows similar behavior, but the pattern is not as pronounced. The gains in the self-excited case (long tube) are lower by 35-130% than those in

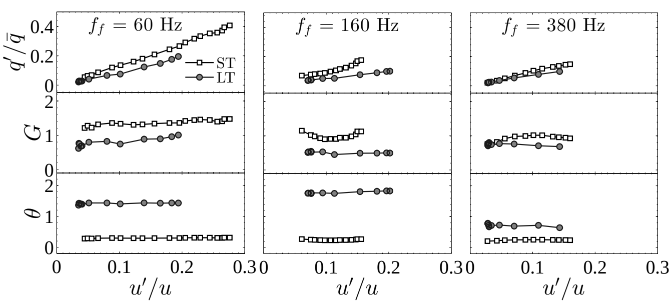

Figure 5: FDFs obtained for long (solid circles) and short (open squares) tubes for u = 10 m/s and three forcing frequencies. Top: normalized heat release fluctuation. Middle: gain. Bottom: phase difference in multiples of π.

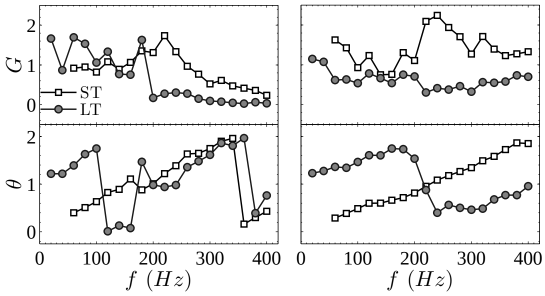

Figure 6: FTFs obtained for the long (solid circles) and short (open squares) tubes for (left) u = 5 m/s, and (right) u = 10 m/s. Top: gain. Bottom: phase difference in multiples of π.

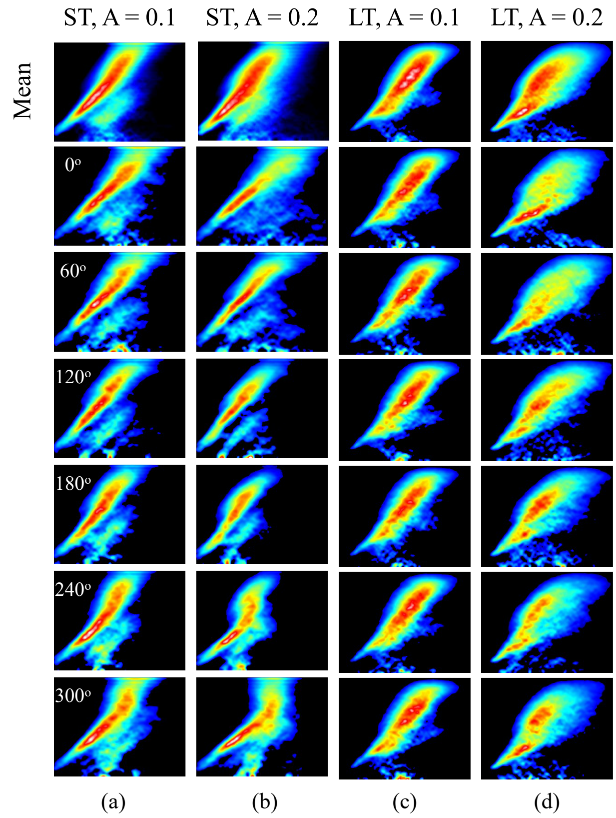

Figure 7: Phase-averaged Abel inverted chemiluminescence images for high power case (u = 10 m/s) forced at 60 Hz. (a, b) short tube, (c, d) long tube. (a, c) A = 0.1, (b, d) A = 0.2. Top row: time-averaged images. Only the upper half of the deconvoluted images are shown. The intensity is displayed in linear pseudo color scale with white denoting the highest intensity and black denoting the lowest. The intensities of images are normalized based on the maximum of each image sequence. (Figure is provided in color online.)

the non-self-excited case (short tube), while the differences in phase between the two cases vary from 0.12π at 380 Hz to 0.50π at 60 Hz (recall that the phase is wrapped at 2π). The largest percentage gain differences occur for 160 Hz forcing, which is close to the self-excitation frequency of 195 Hz. These also correspond to the largest changes in relative phase (0.95π). Significant changes to the flame shape are observed when forcing around this frequency [13].

Finally, we consider the effect of the self-excitation on the FTFs, which are examined over the entire range of forcing frequencies at the lowest forcing amplitudes, both for the short and long tube (Fig. 6). An extensive discussion of the shape of the short tube transfer function is available in Ref. [20]. There is clearly a significant difference between the transfer functions obtained with self-excitation (long tube, LT) and without self-excitation (short tube, ST), for the low and high power case.

In the low power case (left, u = 5 m/s), for the short tube without self-excitation, the gain increases from around unity to 1.8 at 200 Hz, and then decreases with increasing frequency, whilst the phase increases at approximately constant rate except around 180 Hz, where it dips slightly. Such dips in gain creating a node and change in phase are usually associated with the interference of two time scales, here most likely between the acoustic and swirler transfer function [19, 20]. The gain in the self-excited long tube case varies significantly from that in the short tube, with different values at low frequencies, and a significant decrease past the location of the resonant frequency.

The phase difference between heat release and velocity is even more affected by the self-excitation. In the short tube, the phase difference rises with frequency from a small phase, with a constant slope representing the phase delay between velocity and heat release rate for the self-excitation. The triggering of the self-excitation in the long tube creates a different phase of π at low frequencies, which is followed by a rise at the same slope as the short tube case, up to around 180 Hz, where there is a sudden phase change as the forcing frequency sweeps the self-excited frequency. Beyond that point, the phase gently increases at a similar slope as the case of the short tube without self-excitation.

The overall behavior seems to indicate that the low frequency behavior of the flame is very much affected by the incipient excitation around 165 Hz, even if the forcing is taking place at a much lower frequency. The triggering observed in Fig. 3 affects the behavior of the system significantly, so that the two forcing components (from the self-excitation and the forcing) cannot be considered independent. The very different phasing shows that the pressure and heat release fields also change in the presence of self-excitation, leading to significantly different characteristics.

At high power (Fig. 6, right), the differences caused by self-excitation are even more dramatic. Both the gain and phase are significantly changed from the original short tube values, although the slope of the phase remains between the two cases, indicating a constant time delay between forcing and excitation. The largest change in gain, which is accompanied by a sudden change in phase, arises near the self-excitation frequency of 195 Hz: as the forcing frequency sweeps past the self-excitation frequency, the gain remains constant in the self-excited case, whereas the FDF obtained in the short tube increases in the non-self-excited case (short tube).

The phase behavior can be observed by considering the chemiluminescence images of the short and long tube cases, both excited at 60 Hz, at a given A (Fig. 7). In the short tube Figs. 7 (a), (b), we have a thin flame brush, which is excited only slightly by the axial forcing. The long tube flames (Figs.

7 (c), (d)), are more distributed, and rather immune to excitation at low intensities. At the higher forcing intensity of 0.2, the flame is deformed in a rather different pattern than the short tube case, with more distortion in the radial direction, and a different pattern for the centroid location.

These contrasting behaviors of the system in the presence or absence of self-excitation clearly indicate that two commensurate (or even initially incommensurate) excitations cannot in general be considered to operate independently. As pointed out by [16], the growth of one oscillation can be suppressed in the presence of a faster growing mode. Further, the presence of self-excitations clearly affect the effective boundary conditions experienced by the system by changing the phasing of the excited velocities. In the present case, even incipient self-excitations can be triggered, leading to different behavior than in the case of an isolated system. This behavior is analogous to that of non-linear model oscillators with energy added at frequencies that are resonant or away from resonance – but the complex behavior requires thinking beyond the simple linear models.

4. Conclusions

The question posed in this investigation is whether, in thermoacoustic systems with incipient or existing self-excitations at a given frequency, it is possible to obtain appropriate gain and phase information by applying forcing away from the self-excitation frequency. The experimental investigation is made by varying the forcing frequency and amplitude in the presence of a self-excitation in an open tube containing a premixed flame. The results show that both the gain and phase can be entirely dominated by the behavior of the self-excitation, so that in general it is not possible to extract reliable gain and phase information as if the forced and self-excited modes acted independently and linearly.

The consequences for measurements in confined systems is clear: even in the absence of self-excitation, confined systems can develop a self-excitation triggered by non-resonant forcing, leading to a modification of the system response to the forcing. Measurements of FDFs and FTFs in confined systems therefore need to be carefully controlled for potential triggers and additional frequencies, whenever there is a possibility of self-excitation. In particular, the use of multi-microphone methods, which require long tubes for placement of pressure probes, may create opportunities for self-excitation, which may affect the results, unless the boundaries are non-reflecting or carefully controlled, and the possibility of extraneous self-excitations has otherwise been eliminated.

On the other hand, this study also highlights the complexity of real systems, and the emerging opportunities for changing the overall system response by controlling systems that can exchange acoustic energy, modify the phases and trigger or suppress instabilities. Future work on the identification and analysis of such non-linear systems is clearly needed.

5. Acknowledgments

This work was funded by EPSRC-UK under the SAMULET project (EP/G035784/1). H. Han was supported through a CSC fellowship. The technical assistance of Roy Slater is gratefully acknowledged.

References

[1] L. Rayleigh, Nature (1878).
[2] T. C. Lieuwen, V. Yang, F. K. Lu (Eds.), Combustion instabilities in gas turbine engines: operational experience, fundamental mechanisms and modeling, American Institute of Aeronautics and Astronautics, 2005.
[3] S. Stow, A. P. Dowling, Journal of Engineering for Gas Turbines and Power 131 (2009) 031502.
[4] A. P. Dowling, S. R. Stow, Journal of Propulsion and Power 19 (2003) 751–764.
[5] N. Noiray, D. Durox, T. Schuller, S. Candel, Journal of Fluid Mechanics 615 (2008) 139–167.
[6] B. Cosic, S. Terhaar, J. P. Moeck, C. O. Paschereit, Combustion and Flame 162 (2015) 1046–1062.
[7] E. Motheau, Y. Mery, F. Nicoud, T. Poinsot, Journal of Engineering for Gas Turbines and Power 135 (2013) 092602.
[8] I. R. Hurle, R. B. Price, T. M. Sugden, A. Thomas, Proceedings of the Royal Society of London. Series A. Mathematical and Physical Sciences 303 (1968) 409–427.
[9] B. Higgins, M. Q. McQuay, F. Lacas, J. C. Rolon, N. Darabiha, S. Candel, Fuel 80 (2001) 67–74.
[10] B. Schuermans, F. Guethe, D. Pennell, D. Guyot, C. Paschereit, Journal of Engineering for Gas Turbines and Power 132 (2010) 111503.
[11] W. S. Cheung, G. J. M. Sims, R. W. Copplestone, J. R. Tilston, C. W. Wilson, S. R. Stow, A. P. Dowling, Proceedings of the ASME Turbo Expo (2003).
[12] S. Hochgreb, D. Dennis, I. Ayranci, W. Bainbridge, S. Cant, Proceedings of the ASME Turbo Expo (2013).
[13] S. Balusamy, L. K. Li, Z. Han, M. P. Juniper, S. Hochgreb, Proceedings of the Combustion Institute 35 (2015) 3229–3236.
[14] R. Balachandran, P. Dowling, A, E. Mastorakos, Flow, Turbulence and Combustion 80 (2008) 455–487.
[15] S. Schimek, J. P. Moeck, C. O. Paschereit, Journal of Engineering for Gas Turbines and Power 133 (2011) 101502.
[16] J. Moeck, C. Paschereit, International Journal of Spray and Combustion Dynamics 4 (2012) 1–28.
[17] M. R. Bothien, J. P. Moeck, C. O. Paschereit, Proceedings of the ASME Turbo Expo (2009).
[18] K. Kim, S. Hochgreb, Combustion and Flame 158 (2011) 2482–2499.
[19] Z. Han, S. Balusamy, S. Hochgreb, Journal of Engineering for Gas Turbines and Power 137 (2015) 061504.
[20] Z. Han, S. Hochgreb, Proceedings of the Combustion Institute 35 (2015) 3309–3315.
[21] A. F. Seybert, D. F. Ross, Journal of the Acoustical Society of America 61 (1977) 1362–1370.
[22] F. Guethe, D. Guyot, G. Singla, N. Noiray, B. Schuermans, Applied Physics B: Lasers and Optics 107 (2012) 619–636.
[23] B. Schuermans, F. Guethe, W. Mohr, Journal of Engineering for Gas Turbines and Power 132 (2010) 081501.